Aggregated-fluorescent detection of PFAS with a simple chip

Cheng Fang [1], Jinjian Wu [2], Zahra Sobhani [1], Md. Al Amin [1], Youhong Tang [2, *]

[1.] Global Centre for Environmental Remediation (GCER), University of Newcastle, NSW 2308, Australia.

[2.] Institute for NanoScale Science and Technology, College of Science and Engineering, Flinders University, South Australia 5042, Australia.

[*] Corresponding author: Tel.: 61-8-82012138, E-mail: youhong.tang@flinders.edu.au (Y. Tang)

Abstract

In this study, aggregation-induced emission luminogens (AIEgen) are used for the detection of per- and poly-fluoroalkyl substances (PFAS) including perfluorooctanoic acid (PFOA), perfluorooctanesulfonic acid (PFOS) and 1H, 1H, 2H, 2H-perfluorooctanesulfonic acid (6:2FTS). A solution of acetone-water (solvent) containing AIE-PFAS is first formulated. From this solution, one droplet (1-2 μL) is dropped and trapped into a hole in a chip made of glass slide. When the droplet is exposed to air, both water and acetone can vaporise, but acetone vaporises much more quickly due to its high vapour pressure. Consequently, with the solvent volume shrinking, the concentrations of AIE and PFAS increase in the shrinking droplet while the water percentage increases. At a certain stage of this process, the micelle of PFAS forms, accompanied by AIE aggregation. After completely vaporising and drying on the bottom of the chip-hole, the aggregated AIE features fluorescence, the density of which can be effectively linked to the concentration of PFAS. Thus, a simple sensor is developed for PFAS detection in the range of 0.1-100 μM (41 ppb - 41 ppm for PFOA) within around 1 min using a 1-2 μL PFAS sample.

Keywords: aggregation-induced emission; luminogens; PFAS; chip; surfactant; aggregation

1. Introduction

Around half a century ago, Förster and Kasper observed that the fluorescence of pyrene weakened with increasing concentration. It was soon recognized that this was a general phenomenon for many other aromatic compounds, due to the formation of sandwich-shaped aggregation of excimers and exciplexes. This aggregation is aided by collisional interactions between the aromatic molecules in the excited and ground states [1, 2]. In 2001, Tang et al. intentionally established a system [1, 2] in which luminogen aggregation played a constructive rather than destructive role in the light-emitting process. That is, a series of silole molecules was found to be non-luminescent in the solution state but emissive in the aggregated or solid state. For this novel phenomenon, the authors hypothesised that restriction of the intramolecular rotation process was the cause of the "aggregation-induced emission" (AIE). From that time, various applications of AIE were developed. For example, recently Tang et al. reported the detection of a critical micelle concentration (CMC) of surfactants using AIE luminogen (AIEgen) [3]. The idea is that when surfactants reach their CMC, micelles nucleate with hydrophobic cores, where lipophilic AIE can aggregate and subsequently turn on the emission. This is interesting and deserves further research.

Per- and poly-fluoroalkyl substances (PFAS) comprise a family of compounds synthesised by humans [4-7]. PFAS generally contain multiple F-C bonds which lead to their unique properties, such as simultaneous hydrophobicity and oleophobicity, that have not been evidenced from other compounds [5]. PFAS have subsequently been used in many industries including clothing, upholstery, carpeting, painted surfaces, food containers, cookware and fire-fighting foam [4-7]. Unfortunately, the F-C bond is among the most stable covalent bonds and highly resistant to natural degradation (USEPA 505-F-14-001). As a major consequence of their widespread use, coupled with their high persistence, they are currently detected globally, from the North Pole to the South Pole in virtually all life forms and environments [8-11]. Specifically, PFAS surfactants of perfluorooctanoic acid (PFOA) and perfluorooctanesulfonic acid (PFOS) have been documented as having toxic effects on human beings and are listed by various organizations as emerging contaminants [12, 13]. Their monitoring is thus urgently needed [14].

In this study, we explored the interactions between AIEgen and surfactants, particularly PFAS surfactants. AIEgen and PFAS surfactant were dissolved in a solvent of acetone-water, at which time no emission was observed. A small volume of the solution was dropped in a hole in a chip and allowed to dry. The solvent vaporised easily, particularly that containing acetone, due to

its high vapour pressure. As a result, the amount of solvent decreased steadily while the concentration of the AIE-PFAS and the percentage of water simultaneously increased. At a certain stage, the PFAS surfactants reached their CMC and formed micelle [3]. When micelles formed, they could trap AIEgen towards aggregation and enable the AIEgen emission to turn on. Thus, the density of emission corresponded with the micelle density, which corresponded with the concentration of PFAS surfactant in the initial solution.

Perfluorooctanoic acid (PFOA) ammonium salt, perfluorooctanesulfonic acid (PFOS) potassium salt and 1H, 1H, 2H, 2H-perfluorooctanesulfonic acid (6:2FTS) were selected as PFAS in this study. Those anionic PFAS surfactants have attracted much attention recently and have become the main concerns relating to PFAS contamination [15-19]. For interference testing, dodecylbenzenesulfonic acid sodium salt (SDBS), a linear alkylbenzene sulfonate (LAS) was chosen [20-22].

2. Experimental

2.1 Materials

All chemicals, namely acetone, tetrahydrofuran (THF), acetonitrile, PFOA, PFOS and SDBS, were purchased from Sigma-Aldrich (Australia); 6:2FTS was purchased from SynQuest Laboratories, Inc. (USA). All the chemicals were used directly without further purification. Only polypropylene containers / pipette tips were used throughout for the experiments documented in this study [23]. Milli-Q (MQ) water was used (> 18 MΩ•cm) in the present study. All samples were diluted in MQ water in polypropylene centrifuge tubes without pre-treatment unless indicated. All the experiments were carried out at room temperature (~25 °C). Here, two typical AIEgens, tetraphenylethene (TPE) and hexaphenylsilole (HPS) were used. They were synthesised according to references [1, 2].

2.2 Preparation of the chip

A glass chip with a hole array was fabricated at the Australian National Fabrication Facility (ANFF, South Australia Node, Australia). The dimensions of the hole were diameter 2 mm and depth 0.5 mm, so that the chamber volume was ~1.5 μL, as shown in Figure 1. The chip was washed with acetone, ethanol, and then dipped into Piranha solution (2:1 H_2SO_4:H_2O_2, v/v) to

remove all possible organic contaminants. The chip was finally washed with MQ water and dried with nitrogen blow.

Generally, the adsorption of PFAS on a glass surface is striking. However, a plastic chip printed by 3-D printer was tested initially but failed due to the presence of acetone in the solvent. On the other hand, in the presence of acetone, the adsorption of PFAS on a glass surface is weak and can be ignored [24]. Therefore, a glass chip was developed in this study.

2.3 Characterisation and evaluation

AIEgen and PFAS were dissolved in an acetone-water solution at different concentrations as indicated in the following. 1-10 μL of the solution was dropped into a hole in the chip and allowed to dry in air in a fume hood, which usually took 1-10 min, depending on the nature and amount of the solvent, particularly the vapour pressure of the organic part. After drying, the chip was read under a fluorescence microscope (Olympus BX41) under Hg-lamp illumination (U-RFL-T). A filter of WU was selected (dichroic mirror DM400, excitation filter BP330-385, barrier filter BA420). Similarly, the in-situ monitoring drying process was carried out under the same conditions except that the amount of solution was 10 μL for image-taking.

The conductivity of the solution was measured using a LAQUA pH/conductivity meter (PC1100, Horiba, Japan). The photoluminescence (PL) spectra of the silole solutions were recorded on a Cary Eclipse Fluorescence spectrophotometer (Agilent Technologies, USA). Scanning electron microscopy (SEM) (Quanta 450, FEI, USA) was used to characterise the surface topography after dropping and drying of the sample on the silicon surface.

2.4 PFAS analysis

PFAS samples were analysed using an astkCARE™ app (CRC CARE, Australia) [22, 23] when necessary, validated by HPLC-MS (Agilent 1260 + Quadrupole 6130), as reported in references [10, 16, 22]. Generally, the astkCARE™ app testing requires a 10 mL aqueous sample to be mixed with 7 mL of astkCARE™ reagent, using ethyl acetate as an organic solvent and ethyl violet as a dye, in a 25 mL container. After shaking for ~10 sec and then being held stationary for 1-2 min, the top layer of the non-aqueous phase extracted the ion-pair consisting of cationic dye and PFAS anionic surfactants. The intensity or hue of the colour could be correlated with the surfactant concentration level in the initial aqueous solution. As an improved version of MBAS [25], a detection limit of 10 ppb was reached [22].

For HPLC-MS analysis, the standard method (EPA/600/R-08/092) was followed [26]. In general, a 10 μL sample solution was injected into an Agilent 1260 high-performance liquid chromatograph fitted with an Eclipse plus-C18 column kept at 40 °C with the following dimensions: 4.6 mm internal diameter, 100 mm length and 3.5 μm particle size. The flow rate was 0.5 mL/min for the gradient mobile phase of methanol and 5 mM aqueous NH_4Ac for separation. Quadrupole 6130 detector was maintained under negative mode for scanning. Extraction of the molecular ions was conducted at *m/z* 413 for PFOA and 499 for PFOS, respectively. Quantification was carried out by producing a calibration curve using standard solutions (external) of PFOA and PFOS (only linear isomers) with correlation coefficients higher than 0.99 and limit of detection ~0.2 ppb (signal: noise > 3). Blank samples of HPLC-grade MQ water and methanol were run prior to each set of tests to minimise any background contamination that might originate from the Teflon components of the HPLC instrument itself. The nebulizer gas (nitrogen) pressure was set at 35 psi, drying gas flow rate was 10 L/min and temperature was set to 350 ºC, and the capillary voltage was + 3500 V [27]. At least 3 samples were run in parallel for each test for quality assurance and quality control (QA/QC) [11], i.e., 1 blank sample and 1 standard sample for control and 1 sample or 1 batch of samples with different concentrations for testing.

3. Results and discussion

3.1 Sensing mechanism

Figure 1(a) shows a schematic drawing of a micelle when acetone vaporises and water dominates the solvent. That is, in the beginning, the solvent was formulated with 75% acetone and 25% water, in which both TPE and PFOA were well dissolved. Because water and acetone exhibit different vapour pressures of 3.2 kPa and 30.6 kPa respectively at 25 °C, acetone vaporises much more quickly than water when exposed in air. The water fraction increased progressively in the residual droplet while the droplet volume decreased. Consequently, the evaporation triggered two other processes, i.e., (i) PFOA was concentrated to reach CMC, and (ii) AIEgen was concentrated towards aggregation. In this study, considering the size of a droplet of 1.0 μL and the fast drying-off process about 10-60 s, the AIEgen molecules were trapped and aggregated by the PFOA micelles, as assumed by Tang et al. [3, 28].

The trapped AIE molecules thus aggregated into the hydrophobic cores of the micelles. Consequently, the micelles would be turned on with a help of the fluorescence of the AIEgen. Therefore, the fluorescence under UV illumination could be observed, as shown in Figure 1(b). The higher the concentration of the surfactant PFOA, the more easily micelle formed when the acetone vaporised and the higher the density of the fluorescent spot obtained. If the distribution area could be fixed where the solvent dried, such as the chip-hole bottom used in this study, a comparable fluorescent spot density could be obtained. In the present case, the fluorescent spot density after vaporisation/drying corresponded with the concentration of surfactant PFOA in the initial solution. Therefore, a chip with a hole array containing solution droplets for drying was fabricated and used in this study, as shown in Figure 1(c).

Figure 1(d) shows the PL spectra of TPE depending on the concentration of PFOA in solution. Strong emission is observed when the water percentage is higher than 75%. Restriction of intramolecular rotation is responsible for the fluorescent emission. This finding confirms that the aggregation of AIEgen occurred and formed hydrophobic cores towards the formation of a PFOA micelle, or conversely, the formation of a micelle provided a hydrophobic core favouring AIE aggregation. Figures 1(e) and 1(f) show the solution conductivity depending on the concentration of PFOA, in which an almost-linear relationship is observed, both in the high concentration range as shown in Figure 1(e) and in the low concentration range as shown in Figure 1(f). It is also interesting to notice that the slope in Figure 1(f) is higher than that in Figure 1(e), and this shift occurred from the PFOA concentration of 0.7 mM (and above), suggesting the possibility to form micelle, even in a solvent of water-acetone [28, 29]. This possibility was underpinned when the percentage of water increased and the concentration of PFAS surfactant increased, as occurred during the drying process of a droplet.

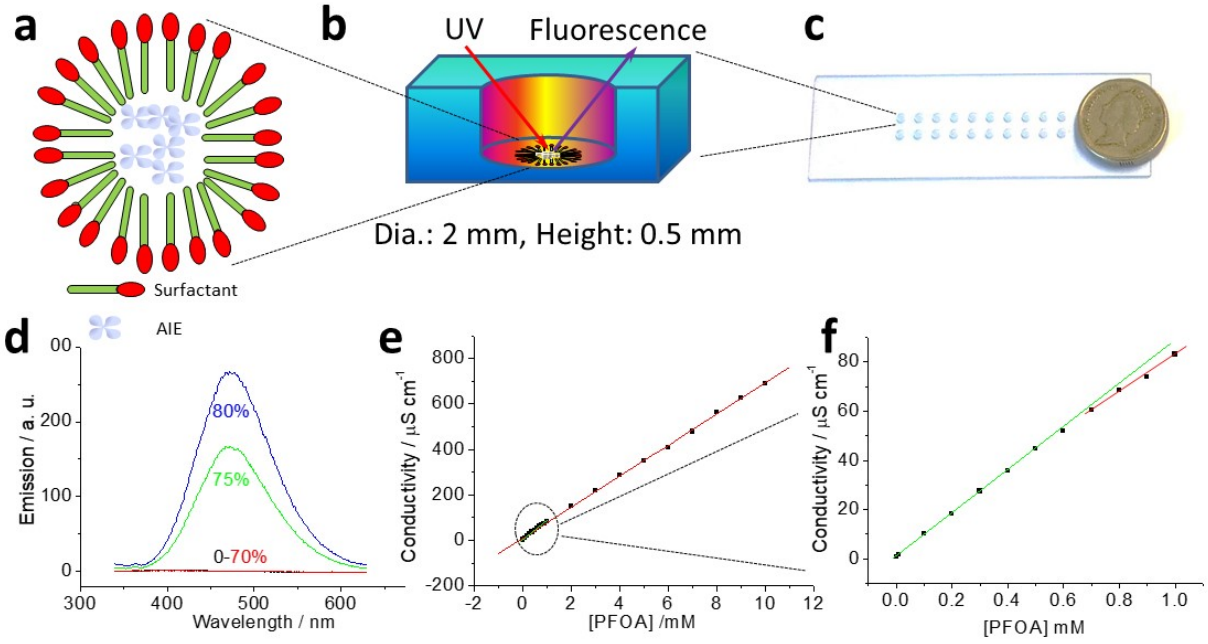

Figure 1. (a) Schematic diagram of aggregate of AIE with the help of micelle, (b) AIE-micelle on the chip-hole bottom, (c) Photo image of a chip with an A$2 coin to show the size, (d) PL spectra of AIE in the presence of PFOA depending on the water percentage mixed with acetone solvent with 10 mM PFOA and 10 μM TPE, (e) Solution conductivity depending on the PFOA concentration in 75% acetone + 25 % water (v/v), (f) zoomed-in area of (e) at the low concentration range.

Figure 2(a) shows in-situ monitoring of the drying process of a droplet. The wires originate from the PFOA micelles and the fluorescence originates from the aggregated TPE molecules. That is, the TPE molecules are aggregated to turn on the fluorescence of micelles of wires. The dark areas feature no fluorescence, thus indicating an absence of aggregated TPE, although the concentration of TPE or PFOA could be high. The high concentration of TPE is unable to aggregate due to the absence of nuclei, whereas the high concentration of PFOA can form micelles but still cannot be turned on due to the absence of aggregated TPE.

The turned-on wires were observed with brighter/higher intensity at the air/solution boundary than in the bulk solution, as shown in Figure 2(a), suggesting that TPE was more likely to be trapped at the boundary than in the bulk solution [30]. That is, PFOA formed micelle/wires first along the boundary and tailing into the bulk solution, to provide the hydrophobic cores

and to trap and concentrate the lipophilic TPE molecules from the bulk solution towards aggregation, to turn on the fluorescence [3].

As already stated, in the dark area along the boundary the concentration of TPE might be high. However, the absence of PFOA micelle means that there are no nuclei for TPE aggregation, which hampers the turning-on. In the dark area in the bulk solution, PFOA micelle might be present. However, the TPE has not yet been trapped/aggregated, which also hampers the turning-on of fluorescence. The trapping/aggregating occurs along the micelle wires' tailing ends into the bulk solution with blurring fluorescence, supporting the assumption that the PFOA forms micelle which provide a hydrophobic core leading towards TPE aggregation.

Actually, micelle was recently reported as a well-known template for the fabrication of nanowire [30-32]. Figure 2(b) shows an SEM image after a droplet has dried on a silicon surface. Aggregated wires are observed, accompanied by a domain, i.e., a particle, supporting the assumption about the micelle formation in the drying process. Note that, after drying, sub-micrometre sized wires could be visualised as fluorescent spots under a fluorescence microscope, as discussed further.

Whereas the intensity of fluorescence was controlled by the concentration of AIEgen, the amount of micelle was controlled by the concentration of PFOA. In the following study, therefore, the density of fluorescent spots including wires, particles and domains after drying on the hole bottom was counted and linked with the PFOA concentration. Note that in the absence of surfactant PFOA, AIE could also aggregate, given the shrinking droplet and the increasing water percentage. However, without the contribution of the PFOA micelle's hydrophobic cores, the aggregation process would be different, and it would be more difficult to form nuclei to initialise subsequent aggregation.

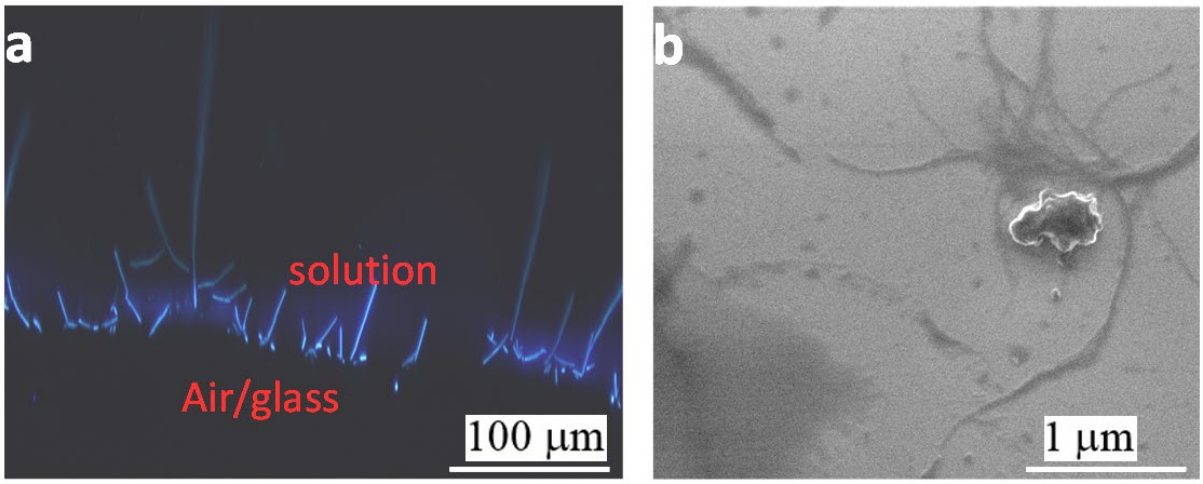

Figure 2. (a) Fluorescent image showing the drying frontier between the solution and air/glass and (b) SEM image after drying. The solution composition was 25% water / 75% acetone containing 10 μM TPE and 10 mM PFOA.

3.2 PFOA detection

Several parameters needed to be optimised towards the detection of PFAS the percentage of water in the water-acetone solvent, AIEgen concentration, droplet size (volume), which were next studied in detail. Figure 3 shows the influence of droplet size (top 3 rows) and the percentage of water (bottom 2 rows) on the PFAS sensing. A droplet of 0.5 μL features a vague result after drying-off (1st row), but the results for 1-2 μL droplets are much better (2nd and 3rd rows). For a 2.0 μL solution in the current test, 2 droplets of 1 μL solution were dropped step-by-step drop into a hole with the chamber volume of 1.5 μL. Therefore, the 1 μL solution was selected for the subsequent testing. 50% water / 50% acetone produces a poor result (4th row). The possible reason is that the AIEgen had aggregated in this solution even before the acetone vaporised, as suggested in Figure 1(d). Subsequently, the micelle contributed a limited turning-on fluorescence when the acetone gradually vaporised. For a low water percentage solution, such as 10%, the result was not good, since the micelle appeared in the latter stage of evaporation to increase the water percentage prior to reaching the CMC. The latter stage of micelle formation featured difficulty for the aggregation of TPE due to the absence of hydrophobic cores from the micelle. Consequently, the results are similar to that of 50% water/ 50% acetone shown on the 4th row in Figure 3. Thus, 25% water / 75% acetone was selected for the subsequent testing.

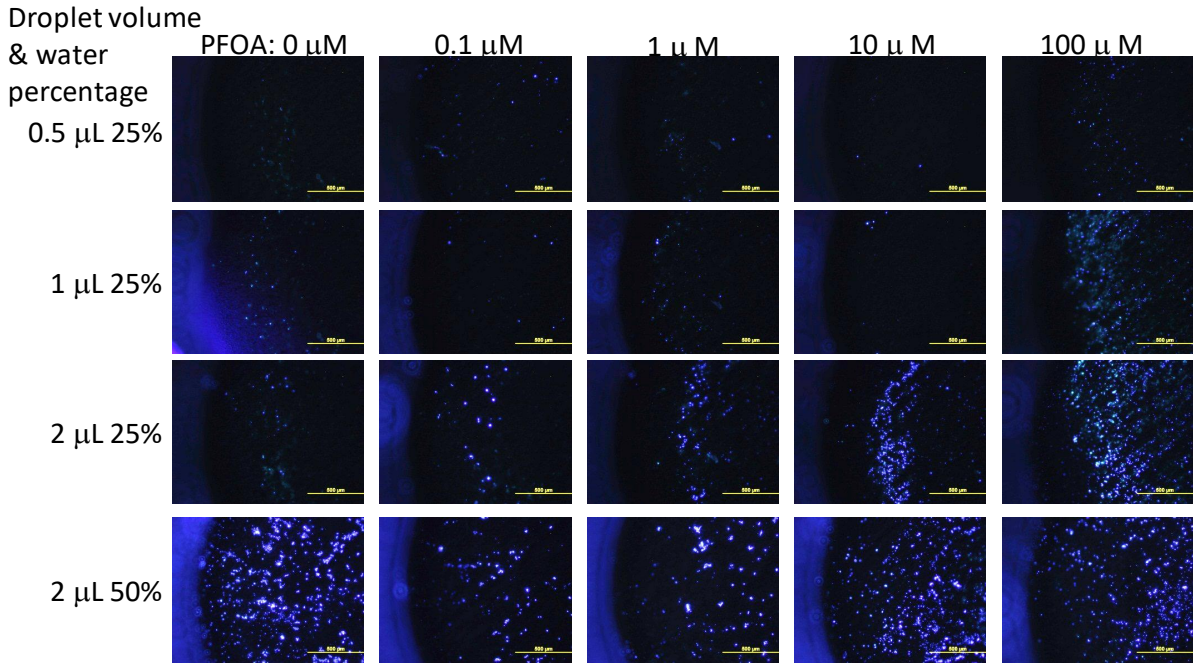

Figure 3. Fluorescent images depending on the droplet volume and the percentage of water in the water-acetone solution (the vertical axis) and the concentration of PFOA (the horizontal axis). A droplet was dropped into a hole in the chip and dried in air. The TPE was maintained at 10 μM in all solutions. Scale bar is 500 μm.

Because AIEgen is a fluorescent luminogen, its concentration played a key role here, as presented in Figure 4. It can be seen that 10 μM TPE features the best result when compared with the results for 5.0 μM and 2.0 μM. A further increase in the TPE concentration led to an unclear background (0 μM PFOA, not shown). 10 μM TPE was selected for the next test.

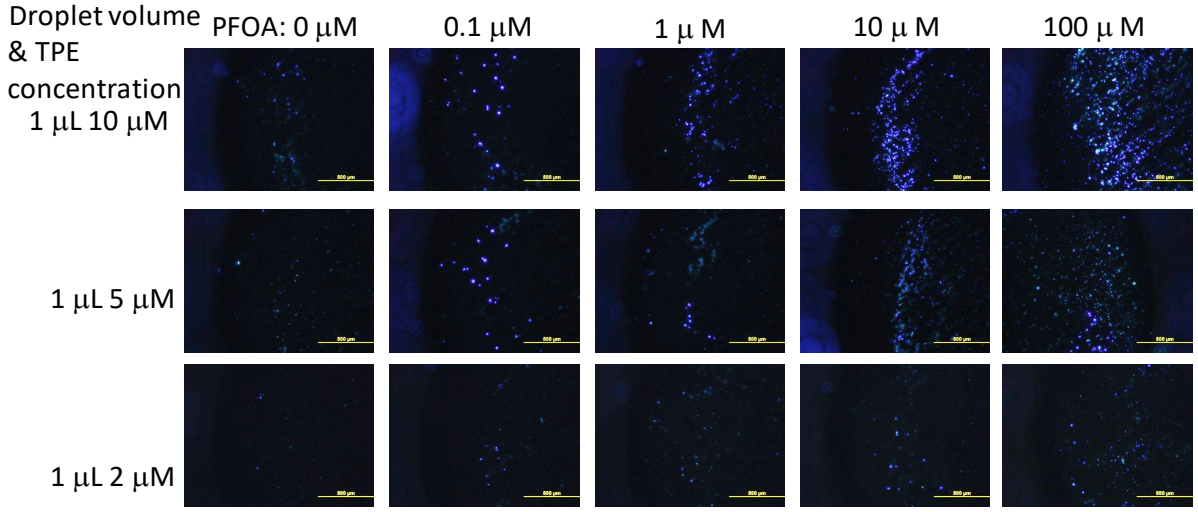

Figure 4. Fluorescent images depending on the concentration of TPE. The solution composition was 25% water / 75% acetone and 1.0 µL droplets were dried in the array holes.

Figure 5 presents the results under the optimised conditions of 75% acetone / 25% water solvent, 10 µM TPE for a fluorescent luminogen to test the PFOA concentration of 1.0 µL droplets of solution drying in holes with 2 mm diameter of. Here, the central part of the bottom of the hole, as the typical part, is shown and read for detection to avoid 'coffee ring interference' [33]. The spot number was counted in the pictured area of ~0.14 mm^2. From the dependence of the spot number on the PFOA concentration, 0.1 µM PFOA was successfully detected (three times the counting variation on the control, 0 µM PFOA).

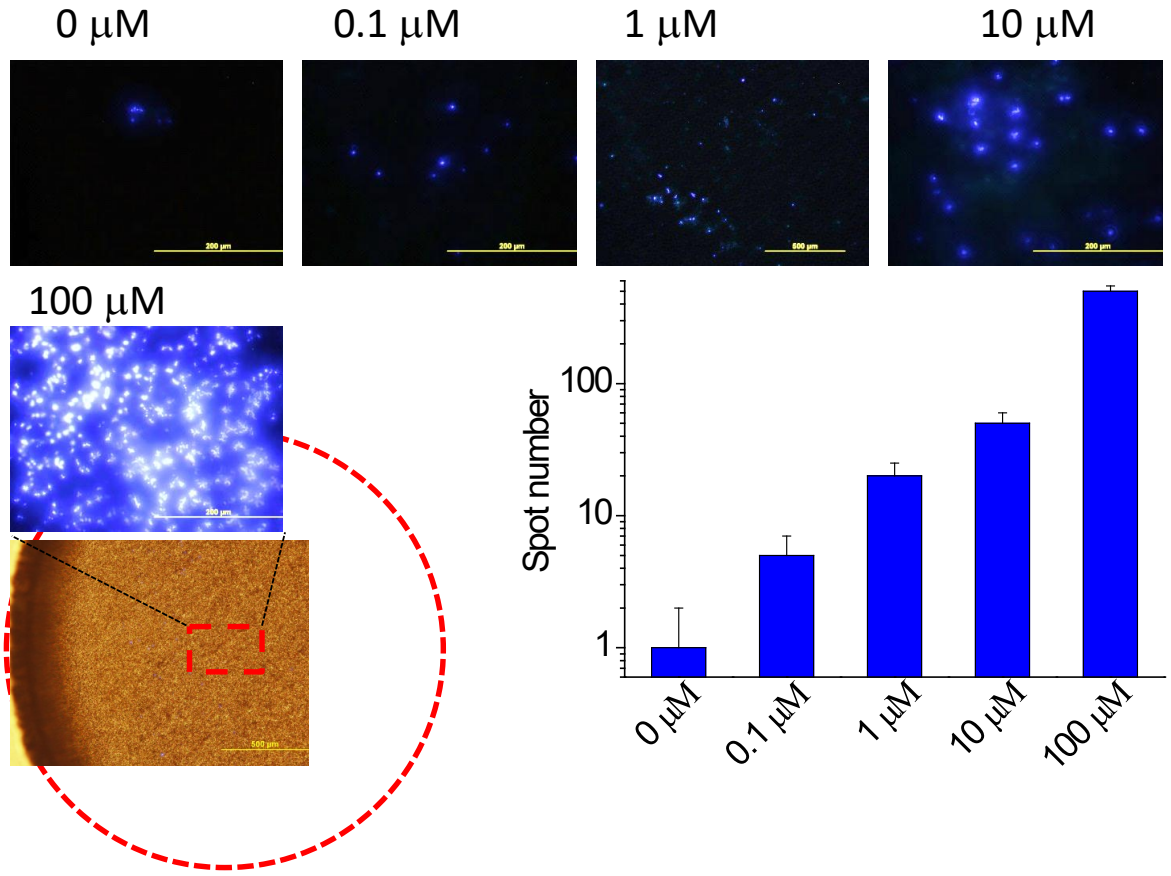

Figure 5. Fluorescent/photo images and spot numbers (reading by ImageJ) depending on the concentration of PFOA (validated by astkCARE app). The solution composition was 25% water / 75% acetone; A1.0 µL-droplet was dried in the chip-array hole and TPE was kept at 10

μM. Scale bars are 200 μm for fluorescent images and 500 μm for photo image. The picture position and the hole size are indicated.

3.3 Other PFASs and SDBS

Figure 6 shows that the study was expanded to other anionic surfactants, namely PFOS, 6:2FTS and SDBS. SDBS is not a PFAS but it still shows similar surfactant behaviour, supporting the aforementioned hypothesis for the trapping of AIEgen for aggregation during the acetone vaporising process.

Admittedly, the selectivity of the PFAS detection is thus questioned, which should be researched further. However, in this study, the hypothesis of a chip-AIE based approach towards the detection of FPAS, or more accurately, anionic surfactant, has been confirmed and developed. Consequently, cationic surfactant might be detected as well, as soon as the micelle can be formed to provide hydrophobic core, to trap AIEgen and to turn-on fluorescence, which also need further research.

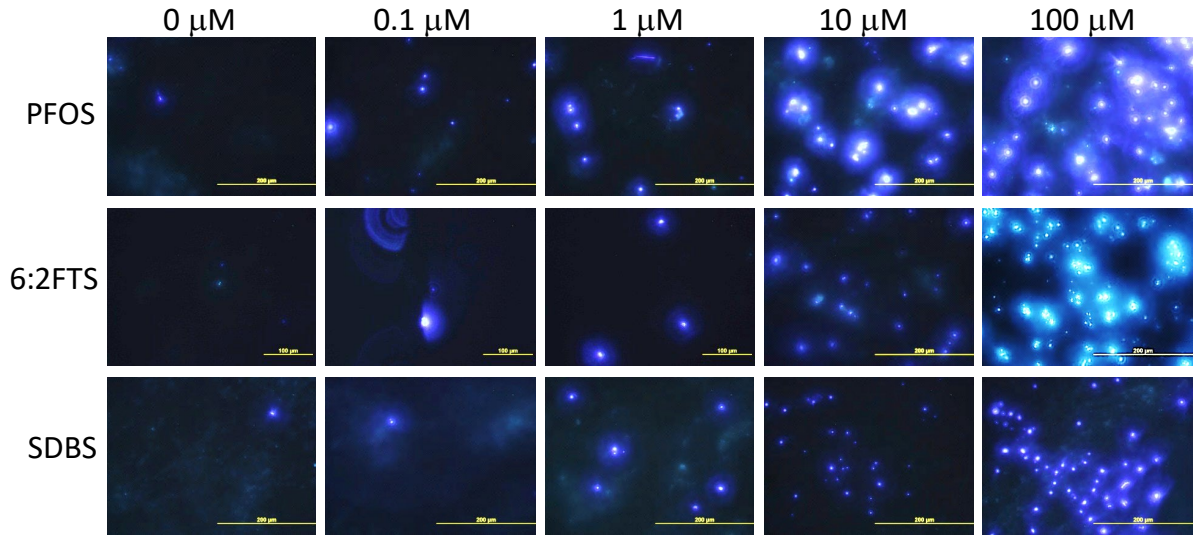

Figure 6. Responses of other AFFFs. The solution composition was 25% water / 75% acetone; A 1.0 μL-droplet was dried in the array hole and the TPE was kept at 10 μM. Scale bars are 200 μm.

3.4 Other AIEgens

To further confirm the aforementioned assumption, HPS, another typical AIEgen, was used as the fluorescent luminogen for study and Figure 7 shows the results. Here the luminogen concentration was decreased from 10 μM to 2 μM due to different molecular configurations and aggregation properties [1, 2]. Similar results can be observed even in different organic component solvents, from acetone, to THF and acetonitrile. The reason those 3 organic solvents were used is that they were easily vaporised in air under different speeds with vapour pressures of 30.6 kPa, 23.5 kPa, 9.71 kPa respectively, at room temperature. The dependence on the concentration of PFOA also suggests the successful detection of PFAS surfactants in this study.

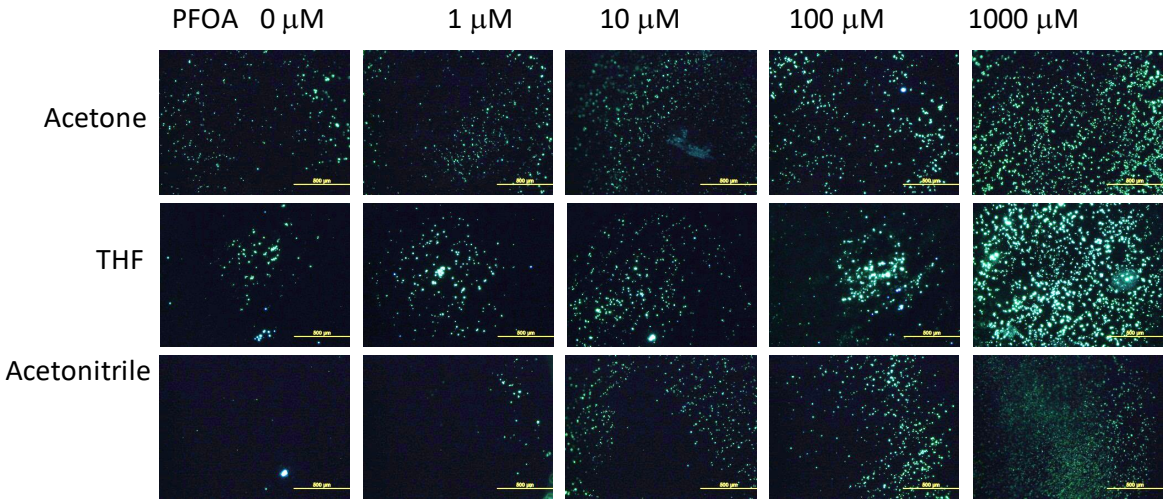

Figure 7. Response of PFOA using HPS as the fluorescent luminogen. The solution composition was 25% water / 75% acetone/THF/acetonitrile; 1 μL droplet was dried in the array hole and HPS was kept at 2 μM. Scale bars are 500 μm.

4. Conclusion

In this study, PFAS in a range of 0.1 μM - 100 μM (41 ppb - 41 ppm of PFOA) was successfully and quantitatively detected using a simple AIEgen as a fluorescent luminogen. Although the sensitivity and selectivity should be further improved, the results are promising and encouraging because a turn-on phenomenon was obtained with a simple operation, i.e., dropping-off and drying within 1-minute, small sample consumption with a volume of 1 μL, and multiplex detection. Whilst HPLC-MS can conduct more accurate test (limit detection of ~0.2 ppb), it is time-consuming (hours) and expensive (>$100/sample). AstkCARE™ app

yields a limit of detection of 10 ppb with help of smartphone and reagents, the sample volume of 10 mL is needed.

Acknowledgements

The authors are grateful for financial support from Defence Innovation Partnership Collaborative Research Funding, South Australia.

References

1. D. Ding, K. Li, B. Liu and B. Z. Tang, Acc. Chem. Res., 2013, 46(11), 2441-2453.
2. J. Mei, Y. Hong, J. W. Y. Lam, A. Qin, Y. Tang and B. Z. Tang, Adv. Mater. 2014, 26, 5429-5479.
3. L. Tang, J. Jin, S. Zhang, Y. Mao, J. Sun, W. Yuan, H. Zhao, H. Xu, A. Qin and B. Z. Tang, Sci. China, Ser. B, 2009, 52(6), 755-759.
4. L. Vierke, C. Staude, A Biegel-Engler, W. Drost and C Schulte, Environ. Sci. Eur., 2012, 24, 16.
5. R. C. Buck, J. Franklin, U. Berger, J. M. Conder, I. T. Cousins, P. de Voogt, A. A. Jensen, K. Kannan, S. A. Mabury and S. P. van Leeuwen, Integr. Environ. Assess. Manag. 2011, 7(4), 513-541.
6. Z. Wang, I. T. Cousins, M. Scheringer, R. C. Buck and K. Hungerbuhler, Environ. Int., 2014, 70, 62-75.
7. Z. Wang, I. T. Cousins, M. Scheringer, R. C. Buck and K. Hungerbuhler. Environ. Int., 2014, 69, 166-176.
8. G. Codling, A. Vogt, P. D. Jones, T. Wang, P. Wang, Y. Lu, M. Corcoran, S. Bonian, A. Li, N. C. Sturchio, K. J. Rockne, K. Ji, J. Khim, K. E. Naile and K. P. Giesy, Chemosphere, 2014, 114, 203-209.
9. E. F. Houtz, R. Sutton, J. S. Park and M. Sedlak, Water Res., 2016, 95, 142-149.
10. S. Taniyasu, K. Kannan, Y. Horii, N. Hanari and N. Yamashita, Environ. Sci. Technol., 2003, 37(12), 2634-2639.

11. P. Wang, Y. Lu, T. Wang, Y. Fu, Z. Zhu, S. Liu, S. Xie, Y. Xiao and J. P. Giesy, Environ. Pollut., 2014, 190, 115-122.
12. EPA, Emerging Contaminants – Perfluorooctane sulfonate (PFOS) and perfluorooctanoic acid (PFOA), in Emerging Contaminants Fact Sheet - PFOS and PFOA, U.S.E.P. Agency, 2014.
13. Z. Wang, I. T. Cousins, M. Scheringer and K. Hungerbuehler, Environ. Int., 2015, 75, 172-179.
14. C. Fang, R. Dharmarajan, M. Megharaj and R. Naidu, Trends Analyt. Chem., 2017, 86, 143-154.
15. R. L. Frost, Q. Zhou, H. He and Y. Xi, Spectrochim. Acta. A Mol. Biomol. Spectrosc., 2008, 69(1), 239-244.
16. B. Boulanger, J. Vargo, J. L. Schnoor and K. C. Hornbuckle, Environ. Sci. Technol., 2004, 38(15), 4064-4070.
17. F. Cheng, Z. Chen, M. Mallavarapu and R. Naidu, Environ. Technol. Innov., 2016, 5, 52-59.
18. C. Fang, M. Megharaj and R. Naidu, RSC Adv., 2016, 6(14), 11140-11145.
19. C. Fang, M. Megharaj and R. Naidu, Austin. Environ. Sci., 2016, 1(1), 1005.
20. B. Weiner, L. W. Y. Yeung, E. B. Marchington, L. A. D'Agostino and S. A. Mabury, Environ. Chem., 2013, 10(6), 486-493.
21. C. A. Moody and J. A. Field, Environ. Sci. Technol., 2000, 34(18), 3864-3870.
22. C. Fang, X. Zhang, Z. Dong, L. Wang, M. Megharaj and R. Naidu, Chemosphere, 2018, 191, 381-388.
23. C. Fang, M. Megharaj and R. Naidu, Environ. Toxicol. Chem., 2015, 34(11), 2625-2628.
24. Z. Du, S. Deng, Y. Bei, Q. Huang, B. Wang, J. Huang and G. Yu, J. Hazard. Mater., 2014, 274, 443-454.
25. A. L. George and G. F. White, Environ. Toxicol. Chem., 1999, 18(10), 2232-2236.
26. J. A. Shoemaker, P. E. Grimmett and B. K. Boutin, EPA 600-R-08/092, US EPA, 2009. Cincinnati, Ohio.
27. C. D. Vecitis, H. Park, J. Cheng, B. T. Mader and M. R. Hoffmann, J. Phys. Chem. A, 2008, 112(18), 4261-4270.
28. N. M. Correa, J. J. Silber, R. E. Riter and N. E. Levinger, Chem. Rev., 2012, 112(8), 4569-4602.

29. Y. Gao, J. Zhang, H. Xu, X. Zhao, L. Zheng, X. Li and L. Yu, ChemPhysChem, 2006, 7(7), 1554-1561.
30. Z. M. Hudson, C. E. Boott, M. E. Robinson, P. A. Rupar, M. A. Winnik and I. Manners, Nat. Chem., 2014, 6(10), 893-898.
31. P. J. Glazer, L. Bergen, L. Jennings, A. J. Houtepen, E. Mendes and P. E. Boukany, Small, 2014, 10(9), 1729-1734.
32. L. Qi, J. Ma, H. Cheng and Z. Zhao, J. Phys. Chem. B, 1997, 101(18), 3460-3463.
33. P. J. Yunker, T. Still, M. A. Lohr and A. G. Yodh, Nature, 2011, 476, 308-311.